Can CAPE Maintain Polar Lows?

TORSTEN LINDERS* AND ØYVIND SAETRA

The Norwegian Meteorological Institute, Oslo, Norway

ABSTRACT

A unique dataset of atmospheric observations over the Nordic Seas has been analyzed to investigate the role of convective available potential energy (CAPE) for the energetics of polar lows. The observations were made during the flight campaign of the Norwegian International Polar Year (IPY) and The Observing System Research and Predictability Experiment (THORPEX) in February and March 2008, which specifically targeted polar lows. The data reveal virtually no conditional instability and very limited CAPE. It is suggested that the significance of CAPE values should be assessed by calculating the time scale t_{CAPE} that is necessary for the heat fluxes from the ocean to transfer the corresponding amount of energy. Even the largest CAPE values have a t_{CAPE} of less than 1 h. These CAPE values are associated with unconditional instability. It is concluded that the observed CAPE should be seen as a temporary stage in an energy flux rather than as an energy reservoir. Based on the findings in this investigation, it is proposed that significant reservoirs of CAPE over the marine Arctic atmosphere are impossible since CAPE production will automatically trigger convection and CAPE is consumed as it is produced.

1. Introduction

Conditional instability has been called upon to explain different types of atmospheric cyclonic activity, at least since the 1940s. McDonald (1942) reports on radio soundings in August 1940 from Swan Island in the Caribbean that "tremendous amounts of energy were potentially available in a state of conditional instability." The concept of convective available potential energy (CAPE) has been used as one measure of how favorable the atmospheric state is to the formation of tornadoes over land, tropical cyclones over the low-latitude ocean, and polar lows over the high-latitude ocean (Holton 2004; Rasmussen and Turner 2003). Today, CAPE and its negative counterpart of convective inhibition (CIN) are used operationally in the United States to asses the risk of extreme wind strengths.

Charney and Eliassen (1964) introduced the theory of conditional instability of the second kind (CISK) for tropical cyclones. They proposed that the energy for such systems comes from the convergence of conditionally unstable air masses, with CAPE being released by the strong updraft in the cyclone. When polar lows began to be more systematically studied, their similarities to tropical cyclones were noted. This led to the suggestion that CISK can work as a mechanism for polar lows (Rasmussen 1979). It was argued that although the high-latitude atmosphere is usually much more stable than in the tropics, outbreaks of cold air from the land or ice-covered parts of the ocean to the open ocean can lead to significant conditional instability. Several following investigations concluded that CISK could contribute to some polar low developments (Craig and Cho 1988; Økland 1987).

Emanuel (1986) introduced the theory that was later named wind-induced surface heat exchange (WISHE). He argued that the intensification and the maintenance of tropical cyclones depend exclusively on self-induced heat transfer from the ocean. Xu and Emanuel (1989) argue that CISK is a problematic explanation for tropical cyclones, since the tropical atmosphere is not particularly conditionally unstable but is nearly neutral to moist convection. The reasonable conclusion is that any sizable amount of CAPE is quickly consumed by convection. Craig and Gray (1996) simulated tropical cyclones and polar lows in an axisymmetric numerical model. They found that the cyclone intensity increased if the surface heat transfer coefficients were increased and

* Current affiliation: University of Gothenburg, Gothenburg, Sweden.

Corresponding author address: Øyvind Saetra, The Norwegian Meteorological Institute, P.O. Box 43, Blindern, 0313 Oslo, Norway.
E-mail: oyvind.saetra@met.no

decreased if the surface drag coefficient were increased. In the latter case, the increased convergence should, according to CISK, have led to intensification. In textbooks WISHE is usually treated as the state-of-the-art theory for tropical cyclones (see, e.g., Holton 2004).

Recently WISHE has been challenged in several papers by Michael Montgomery and Roger Smith and others (Smith et al. 2008; Van Sang et al. 2008; Montgomery et al. 2009). While acknowledging that WISHE has contributed significantly to our understanding of tropical cyclones, they criticize several of its assumptions, such as axis symmetry and gradient wind balance in the boundary layer. They advance a new theory emphasizing the importance of localized structures with deep convection and strong vorticity, dubbed vortical hot towers.

WISHE has been increasingly popular in the study of polar lows (Emanuel and Rotunno 1989; Gray and Craig 1998). Nevertheless, the standard literature on the subject, *Polar Lows* (Rasmussen and Turner 2003), maintains that CISK is a plausible explanation for many polar low developments (see their section 4.5.1). The main basis for this is the claimed correlation in time and space between CAPE and polar lows. It is stated that "CAPE is *not* consumed as quickly as it is produced by large-scale processes."

Rasmussen and Turner (2003) largely ignore the difference between conditional and unconditional instability. Both of these situations may be associated with CAPE, but only in a conditionally unstable atmosphere does CAPE represent a stored energy reservoir that can be released at a later stage. CAPE in an unconditionally unstable atmosphere represents energy that is already in the process of being released.

Rasmussen and Turner (2003) base their claim of correlation between CAPE and polar lows on very few observations and on the reanalysis of numerical weather models. The CAPE values based on observations are calculated by comparing the buoyancy of lifted air parcels with an ambient atmosphere at a different location. The CAPE values based on reanalysis come from the National Centers for Environmental Prediction (NCEP)–National Center for Atmospheric Research (NCAR) reanalysis dataset. The humidity in this dataset belongs to a variable class such that "although there are observational data that directly affect the value of the variable, the model also has a very strong influence on the analysis value (e.g., humidity and surface temperature)" (Kalnay et al. 1996). Users are instructed to "exercise caution in interpreting the results of the re-analysis." The numerical model used in the NCEP–NCAR reanalysis has a horizontal resolution of approximately 210 km. Such a model cannot describe a polar low, and it seems unlikely that it will with any reliability account for the convection

associated with a polar low. In the case of strong heat transfer from the ocean, this will necessarily result in an apparent buildup of CAPE.

The flight campaign of the Norwegian International Polar Year (IPY) and The Observing System Research and Predictability Experiment (THORPEX), conducted in February and March 2008 over the Nordic Seas, offers new possibilities to verify the theories for polar lows against observations. Note that 106 soundings from the campaign were dropped over the ocean and in an atmosphere with cold air outbreaks, or with polar low developments in the vicinity, or inside polar lows. In this paper, we use the observations from the Norwegian IPY-THORPEX campaign to investigate to what extent CAPE can maintain polar lows. Section 2 describes the observations and the calculations of CAPE and CIN. Section 3 presents in some detail the observations of the most intense polar low occurring during the campaign. Section 4 presents the calculated CAPE and CIN for all of the 106 soundings. Finally, a discussion and summary of the results is given in section 5.

2. Methods

a. Observations

The observations were made during an aircraft campaign in February and March 2008. The campaign was organized by the Norwegian IPY-THORPEX project. This project is a part of the Norwegian contribution to the International Polar Year 2007–08 and is aiming at improved understanding and forecasting of adverse weather in the Arctic. From 25 February to 17 March the DLR Falcon 20 jet aircraft of the Deutsches Zentrum für Luft- und Raumfahrt (DLR) was stationed at the Andøya airport in northern Norway (69°N, 16°E). The campaign was led from the nearby Andøya rocket range and specifically aimed at observations of polar lows. At the rocket range observations and forecasts were continuously monitored by the participating scientists in order to assess the timing and location of possible polar low developments.

During the campaign 15 flight missions were conducted, dropping a total of 147 sondes that successfully reported data back to the aircraft. Ten of these missions (106 sondes) were in situations with cold air coming off the ice edge and where infrared satellite images revealed bands of cumulus convection over the ocean. In many cases polar lows were observed in the satellite images but missed by the aircraft. The reason for this was the need to file in-flight plans with the aviation authorities many hours before takeoff. Decisions therefore had to rely on sometimes inaccurate forecasts. Still, many of the soundings from these flights are representative of the

TABLE 1. Dropsonde sensor specifications.

	Range	Accuracy	Resolution
Pressure (hPa)	1080 to 100	±1.0	0.1
Temperature (°C)	−90 to +60	±0.2	0.1
Humidity (%)	0 to 100	±5	1.0
Horizontal wind (m s^{-1})	0 to 200	±0.5	0.1

ambient air for polar lows. The campaign successfully covered two polar low events. The first of these was observed with three flight missions covering the cyclogenesis, early development, and the mature stage. The polar low developed early on 3 March when two flight missions were conducted, dropping a total of 34 sondes that day. Some of these were taken in ambient air; others were taken in areas of intense deep convection. The third flight was on 4 March when 20 soundings were dropped around the polar low at the mature stage. There are very few polar lows, if any, that have been covered by aircraft observations during their full life cycle from cyclogenesis to the mature stage before landfall. The second polar low developed near Andøya between 15 and 16 March. A flight mission was planned for 16 March but had to be canceled because of heavy snowfall at Andøya airport. The snowfall was actually caused by cumulus clouds connected to this polar low. A new attempt was made on 17 March. In this case the flight plan was slightly too far south compared to the position of the low seen in satellite images. However, 1 or 2 of the 13 soundings hit inside the cyclone while the rest were taken in the ambient air.

The dropsondes used in the campaign were from the NCAR GPS dropsonde system, also known as the Airborne Vertical Profiling System (AVAPS). The sondes measure pressure, temperature, humidity, and horizontal wind and transmit the data back to the aircraft. The sensor specifications are shown in Table 1. The sensitivity of the CAPE calculations to the accuracy of the sensors was tested by increasing the observed temperature and humidity of the lifted parcel by the maximum accuracy values in Table 1. This resulted in increased CAPE values of up to 100 J kg^{-1} for the most buoyant parcels. Qualitatively, the main results were unchanged.

The main data quality control is done with the Atmospheric Sounding Processing Environment (ASPEN) software package from NCAR. A detailed documentation of the quality control algorithms can be found in the ASPEN user manual (Martin 2007). In addition, the vertical soundings were plotted and visually inspected to check that they all looked realistic. The lowest observation was manually discarded in three of the soundings. These observations displayed a temperature jump (positive or negative) on the order of 5°C over only a few meters.

The soundings typically start at approximately 350 hPa, or 7.5 km, and terminate at the ocean surface. The resolution is one observation every half second. This gives a spatial resolution of 5–6 m close to the surface and approximately 50 m at 7-km height. The level of the lowest observation is treated as the nominal surface, which thus on average is 3 m above the true ocean surface. This is lower than can be achieved by radiosondes released from the deck of a large ship, especially if one considers the disturbances created by the ship itself. All height indications are with reference to the nominal surface. When a height level is indicated, the first observation below that level is used. After quality control several observations in each sounding are often discarded. This mostly affects the wind observations, which after quality control typically are less dense than the observations of temperature and humidity.

The SST values in this investigation come from optimally interpolated daily means of the Advanced Microwave Scanning Radiometer for Earth Observing System (AMSR-E) satellite observations. The through-cloud capabilities of the microwave radiometers provide coverage under highly convective systems with many clouds, such as polar lows (see http://www.ssmi.com). SST observations from AMSR-E are available for 71 soundings. These include all of the soundings from the flight missions covering the polar low on 3 and 4 March as well as 9 of the 13 soundings from the flight mission covering the polar low on 17 March.

b. CAPE and CIN

The buoyancy of a lifted air parcel can be found by calculating its virtual potential temperature θ_v:

$$\theta_v = \theta(1 + 0.61r - \mathrm{rl}), \tag{1}$$

where θ is the potential temperature, r is the vapor mixing ratio, and rl is the liquid water mixing ratio. If the parcel is undersaturated its virtual potential temperature will remain unchanged until its relative humidity reaches 100% at its lifting condensation level (LCL). Above the LCL, the parcel's potential temperature increases by condensational heating. This is only partly offset by the density increase caused by the lesser volume of liquid water compared to vapor. The lifted parcels are assumed to be nonprecipitating, carrying their condensational loading with them. The buoyancy B of the air parcel is then calculated as

$$B = \theta_v - \theta_{va}, \tag{2}$$

where θ_{va} is the virtual potential temperature of the ambient atmosphere. The soundings do not measure

liquid content, so rl = 0 for both the ambient atmosphere and the lifted air parcels at their level of origin.

The CAPE is calculated (see, e.g., Holton 2004) by integrating the buoyancy from the level of free convection (LFC), where the buoyancy becomes positive, to the level of neutral buoyancy (LNB), where the buoyancy becomes negative again:

$$\text{CAPE} = \int_{\text{LFC}}^{\text{LNB}} g \frac{B}{\theta_{va}} \, dz, \tag{3}$$

where g is the acceleration due to gravity and z is the height.

For CAPE to be released, the air must be lifted from its level of origin (LO) up to its LFC, overcoming the negative buoyancy below the LFC. This negative buoyancy is CIN. The CIN is calculated as the integral of the buoyancy from the LO up to the LFC:

$$\text{CIN} = -\int_{\text{LO}}^{\text{LFC}} g \frac{B}{\theta_{va}} \, dz. \tag{4}$$

CAPE is thus the integration of one continuous layer of positive buoyancy and CIN is the integration of one continuous layer of negative buoyancy. However, a sounding may show that the buoyancy of a lifted parcel alternates between positive and negative values several times. We handle this in the following manner. When there are several layers of positive buoyancy, separated by negative buoyancy, CAPE is calculated by integration over the layer that produces the largest CAPE value. CIN is calculated by integration of all buoyancy from the parcel LO to that layer. This method requires no smoothing of the data and no manual control either. It may, however, produce a negative CIN value. Negative CIN is arguably a contribution to the CAPE, rather than an inhibition of it.

The buoyancy can vary significantly for parcels from different levels of origin, also within the boundary layer. The parcels closest to the ocean surface are typically more humid and more buoyant. Since the lowest observations (at the nominal surface) in this investigation are usually only a couple of meters above the ocean surface, the difference between these parcels and parcels from higher levels is especially pronounced. Section 4 presents the CAPE and CIN for parcels lifted from the nominal surface. The result for parcels lifted from 250 m is also discussed.

If Eq. (3) shows significant CAPE and Eq. (4) shows that the release of this CAPE is inhibited by significant CIN, the stratification is conditionally unstable. On the other hand, if there is significant CAPE but no significant CIN, the stratification is (unconditionally) unstable.

TABLE 2. General interpretation the atmospheric stratification for different combinations of CAPE and CIN.

	Large CAPE	Small CAPE
Large CIN	Conditionally unstable	Stable
Small CIN	Unstable	Neutral

In both of these cases, there can of course be stable stratification above the LNB. If Eq. (3) shows no significant CAPE the stratification is either neutral or stable. If there is significant CIN, the stratification is stable; otherwise, it is neutral. Table 2 summarizes this general interpretation of the four combinations of CAPE and CIN. However, it should immediately be pointed out that Eq. (4) is generally not well suited to distinguishing between neutral and stable stratification, since the upper integration level is the LFC. The CIN calculated with Eq. (4) is a measure of the convective inhibition of the release of CAPE. To get a general measure of the convective inhibition up to an arbitrary level, all buoyancy up to that level should be integrated.

What values of CAPE and CIN should be considered significant? In a severe storm scenario in North America the positive buoyancy of a surface parcel can be 7–10 K or more, corresponding to a CAPE of $\sim$2000–3000 J kg^{-1} or more (Holton 2004; Craven et al. 2002). In the tropics, the positive buoyancy of a low-level parcel is around 1–2 K over 10–12 km, corresponding to a CAPE of $\sim$500 J kg^{-1} (Holton 2004; Xu and Emanuel 1989). Williams and Renno (1993) include the ice phase when calculating CAPE, assuming freezing at $-10°$C. They get values near 2000–4000 J kg^{-1} for the tropics. Rasmussen and Turner (2003) mention CAPE values near 1000 J kg^{-1} over the Nordic Seas and refer to 400–600 J kg^{-1} as "moderate." The CIN preventing the release of CAPE is typically much lower.

One way of assessing the significance of a CAPE value is to compare it with the sea surface heat fluxes. This is especially relevant with reference to Rasmussen and Turner (2003), since they claim that CISK explains the rapid intensification of some polar lows better than WISHE (p. 399). That claim is intuitively logical, if one assumes that CISK involves the release of CAPE in the form of an energy reservoir already stored in the atmosphere (which Rasmussen and Turner do at least in some instances), while WISHE relies on the self-induced buildup of energy transfer from the ocean.

We suggest that the best way of assessing the significance of a CAPE value, in terms of an energy reservoir, is to calculate the time scale t_{CAPE} that it takes the heat flux from the ocean to transfer the energy corresponding to that CAPE value. By this we do not imply that the (local) sea surface heat flux is the only possible cause of

CAPE, although we believe it is the likeliest candidate. Increased buoyancy may be caused either by the increase of θ_v or by the decrease of θ_{va} [see Eq. (2)]. Regardless of the cause of CAPE, its release competes in significance with the continuous energy transfer from the ocean. If t_{CAPE} is considerably shorter than the lifetime of a polar low, there must be other sources of energy than the release of preexisting CAPE. This energy source can, for example, be the release of *continuously replenished* CAPE.

We start with a simplified version of Eq. (3):

$$CAPE = g\frac{B}{\theta_{va}}H, \tag{5}$$

where H is the height of the convection (LNB − LFC). We further assume that the (positive) B in Eq. (5) can be calculated as

$$B = \frac{Qt_{CAPE}}{Mc_p}, \tag{6}$$

where M is the mass per unit area of the layer that has the CAPE value, Q is the sea surface heat fluxes (sensible and latent), and c_p is the heat capacity at constant pressure. By inserting Eq. (6) into Eq. (5), we get

$$t_{CAPE} = CAPE\frac{Mc_p\theta_{va}}{QgH}. \tag{7}$$

In section 4 we estimate t_{CAPE} by using the CAPE values for parcels lifted from 250 m, since we believe they are more representative for the boundary layer than the parcels at the nominal surface. We further use $M = 1000$ kg m^{-2}, $\theta_{va} = 300$ K, and $H = 3000$ m as representative values.

The sensible Q_s and latent Q_l sea surface heat fluxes can be calculated by the following bulk formulas:

$$Q_s = \rho c_p C_H |V_{10}|(T_{ss} - T_{10}), \tag{8}$$

$$Q_l = \rho L_v C_E |V_{10}|(q_{ss} - q_{10}), \tag{9}$$

where ρ is the density, L_v is the latent heat of vaporization, C_H and C_E are bulk transfer coefficients, and V_{10} is the 10-m wind. Also, $(T_{ss} - T_{10})$ and $(q_{ss} - q_{10})$ are the temperature and specific humidity difference, respectively, between the sea surface and the 10-m level, where T_{ss} is assumed to equal the SST and q_{ss} is assumed to equal saturation at the SST. Values of constants are given in Table 3. The 10-m values are found by interpolation of the sounding data, which is done by assuming logarithmic profiles and by assuming that the last observation (the nominal surface) is situated 3 m above the true ocean surface.

TABLE 3. Constants.

	Value	Units
C_H	1.0×10^3	No unit
C_E	1.2×10^3	No unit
c_p	1004	J kg^{-1} K^{-1}
L_v	2.5×10^6	J kg^{-1}

3. Polar low event 3–4 March 2008

In this investigation all soundings taken during the campaign period are used in the search for finding significant CAPE values over the ocean. However, as the link to polar low maintenance is one key objective, the polar low event observed during three flight missions on 3 and 4 March is of particular interest. Here, we will present some of the observations from these flights and give a short description of the polar low evolution from a disturbance on a convergence zone to a mature polar low.

During a cold air outbreak on 3 March 2008 a front with northerly winds was forming in the Fram Strait between Greenland and Svalbard. At approximately 74°N easterly winds caused a convergence zone where polar low development was expected. Based on the available forecasts, it was decided to launch two flight missions during that day. The first flight took off at 1000 UTC, releasing dropsondes between then and 1330 UTC. The takeoff time for the second flight was 1430 UTC and lasted for 3 h. Based on infrared images it was obvious that a polar low was under development during this flight. During the night the polar low moved in southeast toward the Norwegian coast. A third flight was launched at 1000 UTC 4 March, lasting for a bit more than 3 h. A few hours after this last flight was finished the polar low started to make landfall with the strongest winds on the coast of Trøndelag in Norway.

Figure 1 shows the infrared satellite image valid at 1221 UTC 3 March. At this stage, an Arctic front is seen as a well-defined convergence zone along 0°E, stretching from the sea ice edge down to approximately 75°N. From here it runs eastward along 75°N latitude to approximately 10°E. Evidence of a cold air outbreak west of the low is seen as cloud streets developing downwind of the sea ice edge. Further downwind, more or less parallel to 70°N latitude, an Arctic front is clearly seen marking the area of colliding arctic and polar air masses. The dropsonde positions are marked with numbered squares Fig. 1.

Figure 2 shows the satellite image valid at 1601 UTC 3 March, which is nearly midway into the second flight mission on 3 March that lasted for 3 h. At this moment the cloud formations near the kink in the convergence area, where the northerly flow meets the easterlies at approximately 74°N, indicate that a polar low is in
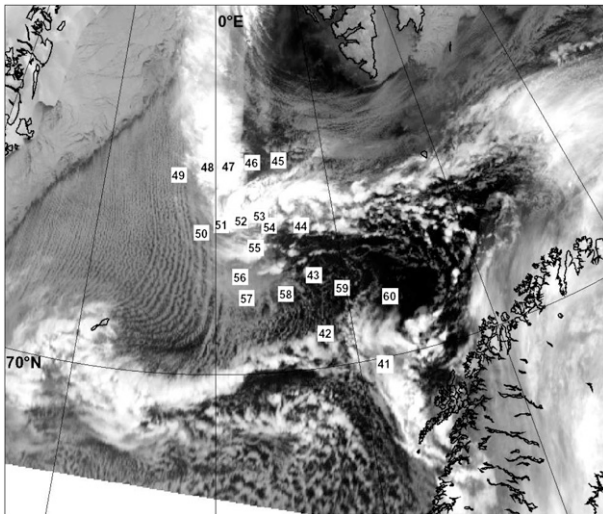
FIG. 1. NOAA satellite image at 1221 UTC 3 Mar. White squares with numbers indicate soundings.
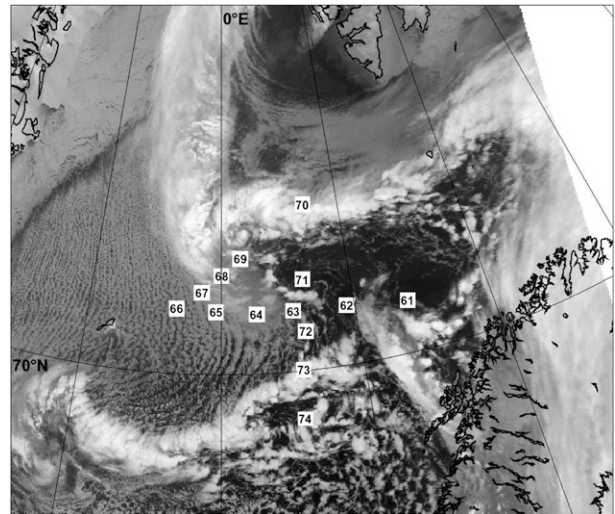

FIG. 2. As in Fig. 1, but at 1601 UTC 3 Mar.

formation. Closer inspection of the satellite image in this area indicates the formation of an eyelike feature surrounded by cyclonic motion. The dropsonde positions are marked with numbered squares in Fig. 2.

Figure 3 shows the polar low at 1128 UTC, approximately midway through the flight mission conducted on 4 March. During the night, the polar low has matured and also intensified, as indicated by both meteorological analyses and scatterometer observations (not shown here). Now the center of the polar low consists of organized convective cells and with a spiral-like cloud band ending as a northward stretching tail, which is the remnant of the convergence zone. The dropsonde positions are marked with numbered squares in Fig. 3.

During the first flight on 3 March, dropsondes were released during four more or less straight legs. The second of these made a section through the Arctic front almost parallel to 75°N latitude (sondes 45–49 in Fig. 1). This is slightly north, and hence upstream, of the area of polar low cyclogenesis. Along this section five sondes were dropped.

Figure 4 shows the wind speed from this section based on the dropsonde data. The distance is given in kilometers along the x axis, where zero, the left side of the plot, is at the west. The positions of the dropsondes are marked as black vertical bars on top of the figure. Figure 5, the observations of potential temperature, reveals a low-level front, confined below the 700 hPa surface with tongue of cold air on the western side. This is usually referred to as reversed shear. The cold-air outbreak event is dominated by northerly winds. Along the north–south-oriented front, the coldest air is found on the western side. The thermal wind balance then requires the geostrophic winds

to decrease with height (Rasmussen and Turner 2003); that is, the wind is expected to decrease with height outside the planetary boundary layer. In the planetary boundary layer, however, friction reduces the wind speed toward the ground, resulting in a low-level jet somewhere in the upper part of the planetary boundary layer. This is clearly seen in Fig. 4, which shows the wind speed along the same section. A wind maximum is observed at 940 hPa under sonde number 3 from the right in Fig. 4, at approximately 130 km, where the observed wind speed was 26 m s^{-1}.

The second flight on 3 March released dropsondes along three straight legs. The second of these made a section near the center of the developing polar low. The polar low at this moment is in its early stage of development. The cyclogenesis takes place in the area where the cold northerly winds and the warmer easterlies converge. A number of investigations have suggested upper-level potential vorticity (PV) anomaly in explaining polar low development (Rasmussen and Turner 2003). In an atmosphere with low static stability, such as the situation during an Arctic cold-air outbreak, a positive upper-level PV anomaly very effectively induces lower-level cyclonic motion. Figure 6 shows the equivalent potential temperature in the section through the cyclogenesis area. In the lower levels of the plot we recognize the shallow front discussed above. A striking feature at higher levels is the downfolding of the equivalent potential temperature surfaces near the center. Warmer air and significantly lower stability are observed between 400 and 800 hPa. These observations are indeed very close to what looks like the cyclone center in Fig. 2. We propose that this may be caused by intrusion
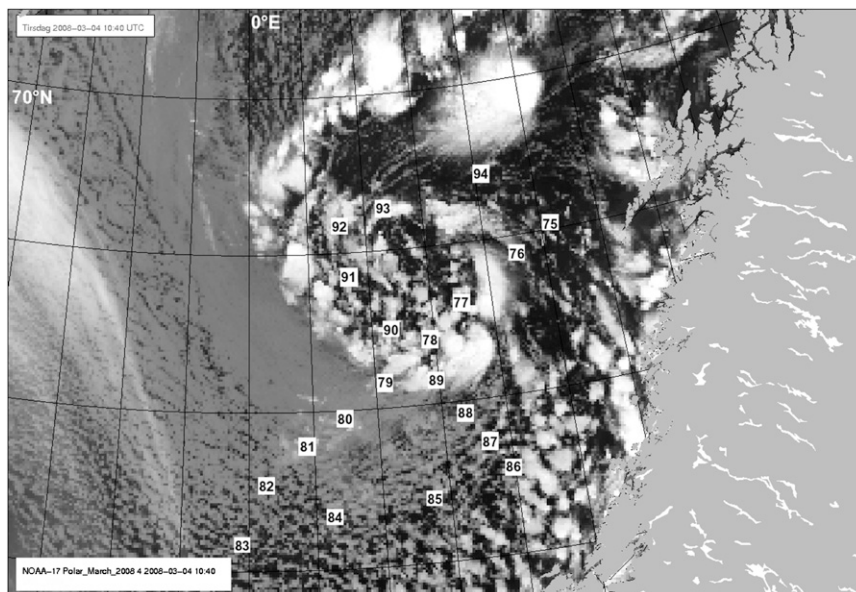
FIG. 3. NOAA satellite image of the polar low at 1127 UTC 4 Mar. White squares with numbers indicate soundings.

of stratospheric air with higher potential temperature than its surroundings.

The next day, on 4 March, the last flight mission into the polar low took off at 1000 UTC, dropping a total of 20 sondes. The first leg was a straight cut through the low in a direction from northeast to southwest (see the marks in Fig. 3). During this flight leg, nine meteorological sondes were dropped. Figure 7 shows the equivalent potential temperature through this section. In this figure southwest is on the right side of the figure. Remains of the shallow front and low-level cold tongue are still visible on the southwestern side of the section. The observations reveal a warm core cyclone with low stability near the cyclone eye. These sondes are numbered 72–74 in Fig. 3 and are the sondes that were dropped closest to the cyclone center according to the satellite image. Figure 8 shows the relative humidity for the same section. At the mature stage the polar low is characterized by towers of moist air. These convective towers more or less penetrate the whole troposphere and relative humidity values above 80% are observed below 500 hPa. A very interesting feature in Fig. 8 is the dry upper-level air found near the center of the cyclone. We interpret this as an intrusion of stratospheric air near the center of the cyclone. This is probably linked to the downfolding of the potential temperature surfaces found in Fig. 6. If this really is an intrusion of stratospheric air, it will have higher potential temperature than its surroundings when it enters the cyclone center. To conserve potential vorticity, the cyclonic motion is intensified. This might be one mechanism that maintains the polar low before it landfalls and fades.

4. Results

Figure 9 shows the CAPE and CIN for parcels lifted from the nominal surface for all soundings. There are only 13 soundings with CAPE values larger than 100 J kg^{-1}. All of these have 0 J kg^{-1} of CIN; that is, their LOs coincide with, or are higher than, their LFCs. [For sounding 89 the CIN value is actually -10 J kg^{-1}; see the discussion after Eq. (4).] Following the general interpretation of the stratification in Table 2, and given that the CAPE values are considered large enough, these soundings show (unconditional) instability. There is not one sounding showing conditional instability.
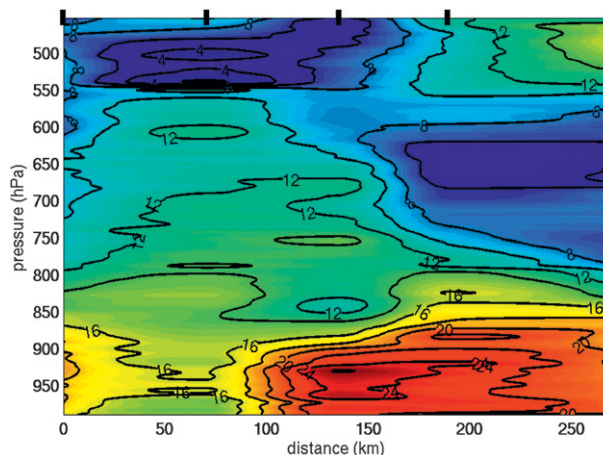

FIG. 4. Total wind speed (m s^{-1}) from dropsondes observations on 3 Mar 2008. Dropsonde positions are marked as black bars on top of the figure. This section is from west to east with west on the right side.
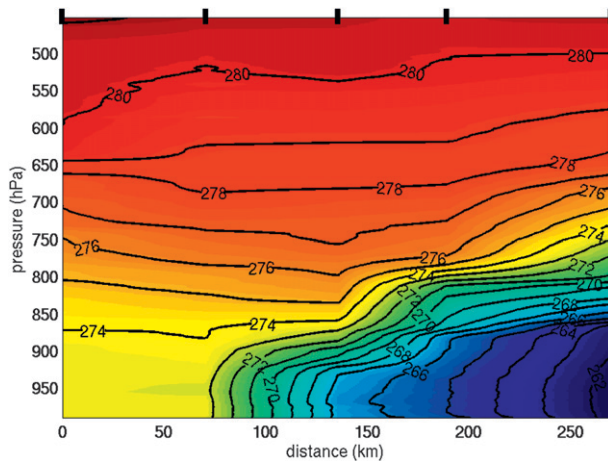
FIG. 5. Potential temperature (K) from dropsonde observations on 3 Mar 2008. Dropsonde positions (45–49 in Fig. 1) are marked as black bars on top of the figure. This section is from east to west with east on the left side.

As an alternative method we also calculated CAPE by including the ice phase and assuming freezing at $-10°C$, as suggested by Williams and Renno (1993). This method yields around 100 J kg^{-1} higher CAPE values (not shown) for the most buoyant parcels. Qualitatively the main results remain the same.

As mentioned in section 2b, the CAPE values for the parcels lifted from the surface are generally a lot higher than that of an average boundary layer parcel. The observed CAPE for parcels lifted from 250 m (not shown) is in none of the soundings significantly higher than the CAPE of the parcels lifted from the surface. In most of the soundings, the 250-m value is a lot lower. Only in sounding 84 is the CAPE value for a parcel lifted from 250 m larger than 100 J kg^{-1}. The CIN inhibiting the release of that CAPE is 0.7 J kg^{-1}.

Of the 13 soundings showing CAPE larger than 100 J kg^{-1}, 10 belong to the polar low of 4 March, observed by soundings 75–94 (see Fig. 3). The remaining three belong to the polar low of 17 March, observed by soundings 135–147 (no satellite image shown). Figure 10 shows the buoyancy profiles for parcels lifted from the nominal surface and from 250 m, for all the soundings of 4 March. Also shown are the sensible and latent sea surface heat fluxes and t_{CAPE}. The positions of these soundings from 4 March are shown in Fig. 3 superimposed on an infrared satellite image from the time of sounding 83. More than two hours pass between the first and the last of the soundings of the mission. The satellite image is thus most representative for the soundings made around that time.

The profiles show that high levels of positive buoyancy for the surface parcels do not usually correspond with similar values for the 250-m parcels. The profiles also
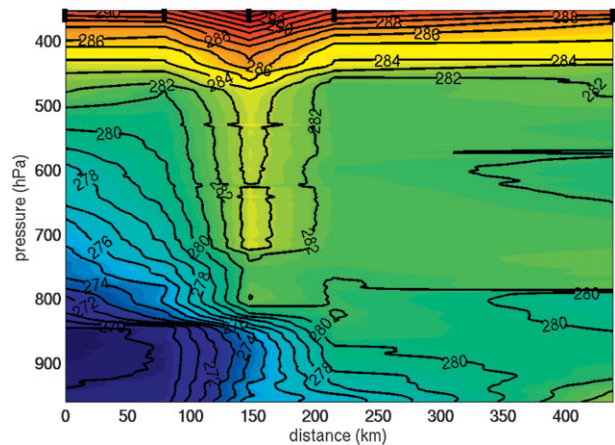

FIG. 6. As in Fig. 5, but for equivalent potential temperature (K).

show the baroclinic structure of the polar low. The low-level cold air to the south and west of the cyclone center creates several cases of strongly buoyant surface parcels, but the strong capping at approximately 2 km limits the highest level of positive buoyancy to that height. In the cyclone center and to its north and east there is no similar capping, which allows the highest level of positive buoyancy to reach over 5 km for the most buoyant surface parcels.

It is easy to see from these profiles that the soundings that show significant CAPE at the nominal surface and 250 m are (unconditionally) unstable, since the positive buoyancy starts already at the parcel LO and is not preceded by any layer of negative buoyancy. This shows that the CAPE values represent energy in the process of being released. If this is a continuous process and not a one-time release of an energy reservoir, one highly plausible source is the sea surface heat fluxes. However, it is not easy to
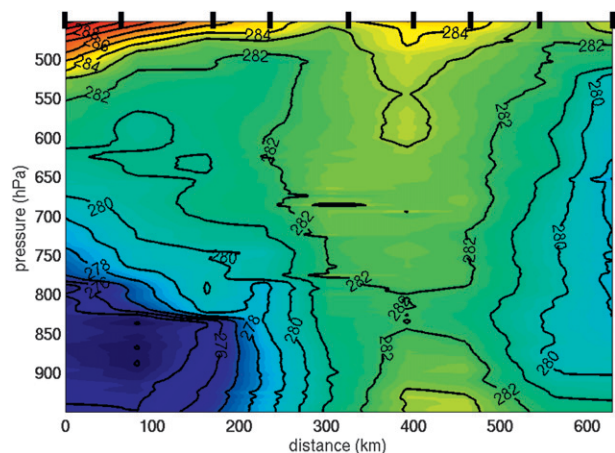

FIG. 7. Equivalent potential temperature (K) from dropsonde observations on 4 Mar 2008. Dropsonde positions (75–83 in Fig. 3) are marked as black bars on top of the figure. The section is from southwest to northeast, with southwest on the right side.
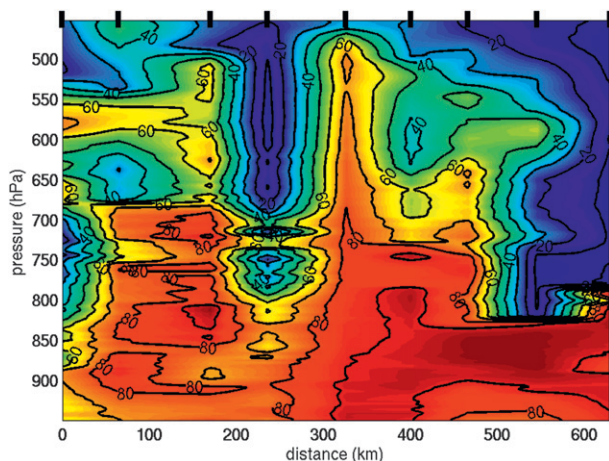
FIG. 8. Relative humidity (%) from dropsonde observations on 4 Mar 2008. Dropsonde positions are marked as black bars on top of the figure. The section is from northeast to southwest, with northeast on the right side.

find any correlation between the heat fluxes and the CAPE values. This can probably be explained by a combination of several factors:

1) A large CAPE is the product of a large positive buoyancy integrated over a large height. Cold low-level air,

such as in soundings 80–85, may cause strong heat fluxes from the ocean and buoyant surface parcels. The surface parcels will, however, only be buoyant within the layer of cold air, and the integrated buoyancy may therefore be moderate.

2) The nominal surface may be anything between 0 and 6 m above the true surface, even with a properly functioning instrument. The soundings frequently reveal a significant jump in both temperature and specific humidity from the second to last to the last observation. This indicates that there may be great variations in buoyancy within the meters closest to the ocean surface.

3) The soundings show a snapshot of a turbulent and fluctuating atmosphere. The CAPE values are equivalent to the energy transfer by the sea surface heat fluxes during only a short time. From a flux perspective CAPE represents a temporary storage of the sea surface heat fluxes. How limited the storage time is can be assessed by t_{CAPE}. In Fig. 10 t_{CAPE} is shown for each of the soundings below the value for the sea surface heat fluxes. If the consumption of CAPE by convection and its creation by the sea surface heat fluxes vary on a time scale comparable to t_{CAPE}, this will lead to great variations of CAPE.
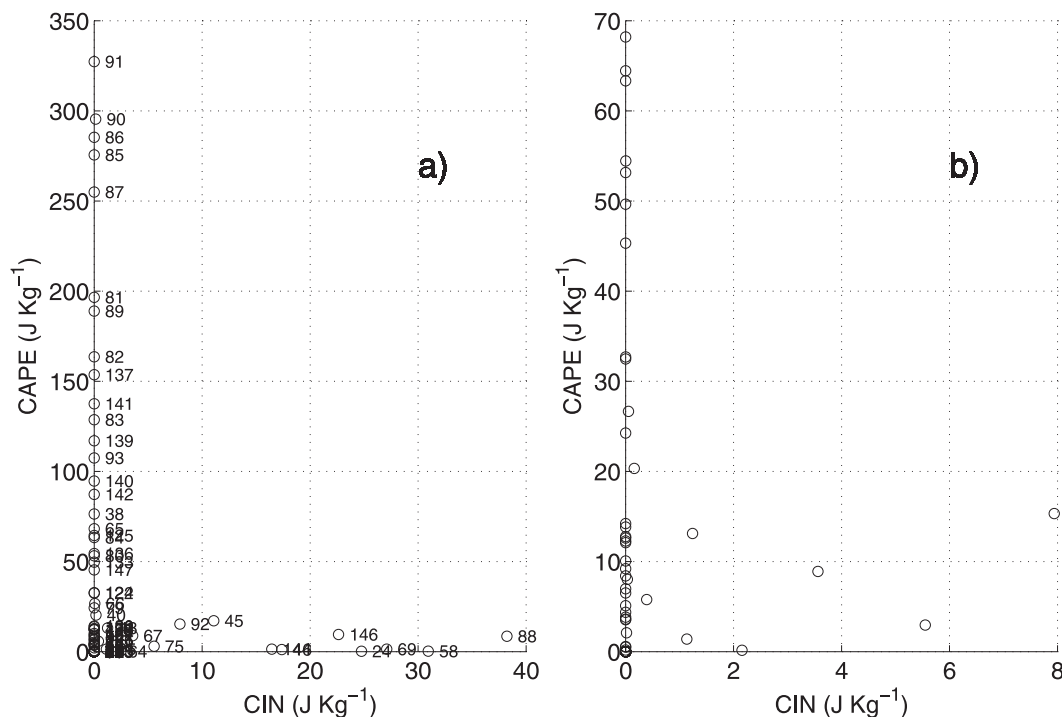

FIG. 9. CAPE and CIN for parcels lifted from the nominal surface: (a) results of all 106 soundings and (b) soundings with low CAPE and CIN values. Sounding numbers are indicated in (a) next to the data points. CAPE values larger than 70 J kg^{-1} have been adjusted with up to ±10 J kg^{-1} to increase readability. The CIN value of sounding 89 has been adjusted from −10 to 0 J kg^{-1}.
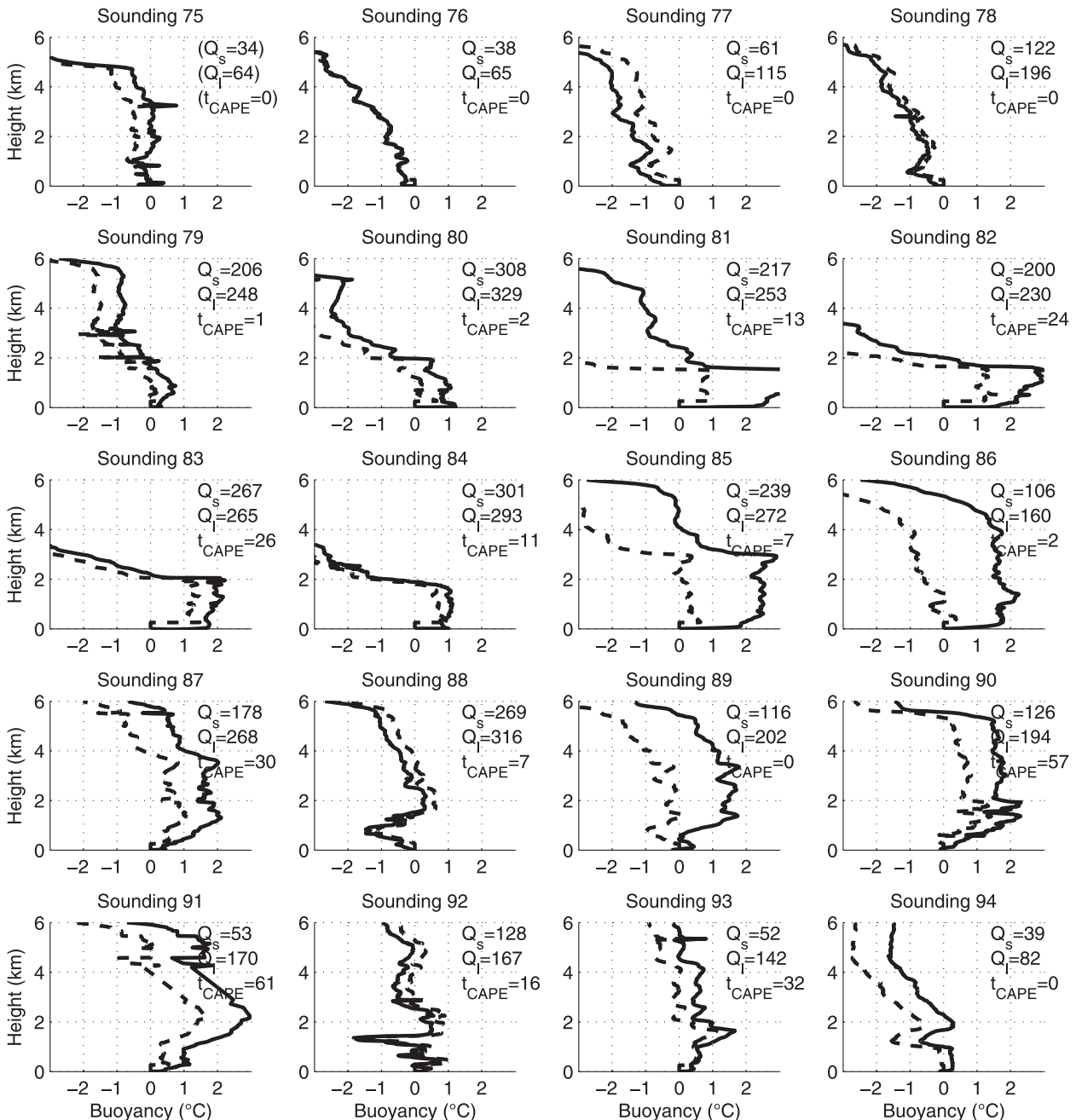
FIG. 10. Buoyancy for the soundings of the flight on 4 Mar. Solid lines are for parcels lifted from the nominal surface. Dashed lines are for parcels lifted from 250 m. The Q_s and Q_l values in the top right corners of each panel are given in watts per square meter. The t_{CAPE} values (min) are calculated using Eq. (7). The values for sounding 75 are in parentheses because the lowest wind observation is more than 500 m above the nominal surface.

The soundings in Fig. 10 were conducted inside and in the vicinity of an intense polar low with accompanying deep convection, clearly visible in Fig. 3. Figure 11 shows corresponding buoyancy profiles for all of the soundings from the two flights on 15 March, which covered the cold air outbreak preceding the polar low of 16 and 17 March.

In these soundings the parcels lifted from the nominal surface and from 250 m have only little positive buoyancy. They are buoyant only in a layer close to the surface and not subject to any convective inhibition.

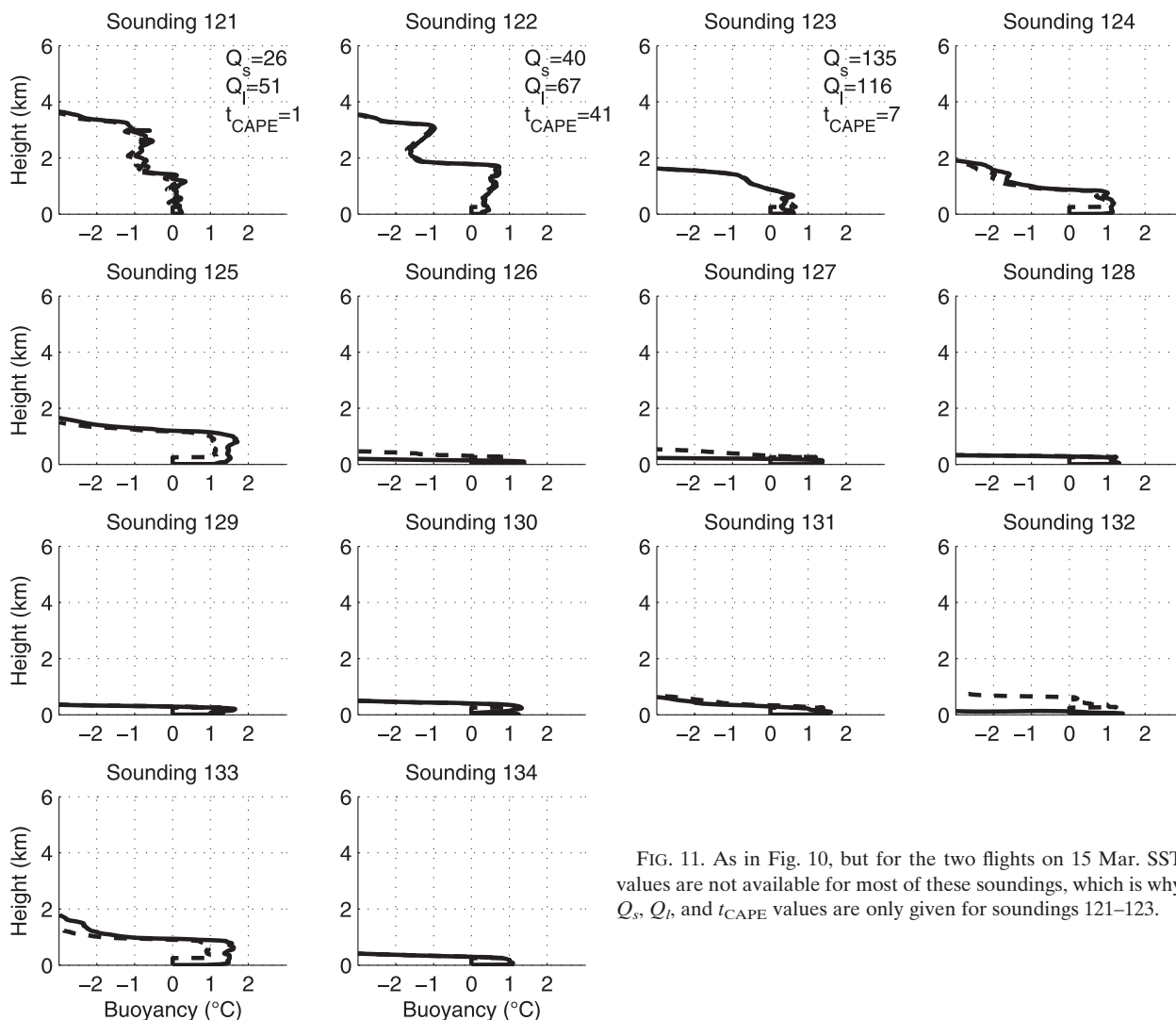We have calculated t_{CAPE} for all of the soundings where SST observations are available. Mostly t_{CAPE} is

FIG. 11. As in Fig. 10, but for the two flights on 15 Mar. SST values are not available for most of these soundings, which is why Q_s, Q_l, and t_{CAPE} values are only given for soundings 121–123.

extremely short and only for sounding 91 is it longer than 1 h (61 min). This leads to an immediate conclusion. One can imagine that the continuous energy transfer from the ocean, which may appear temporarily in the form of CAPE, contributes significantly to the energy budget of a polar low. However, it is hard to imagine that the release of an energy reservoir equivalent of 1 h or less of this energy transfer represents any significant part of that budget, integrated over a longer time.

5. Conclusions and discussion

Polar lows are a complex weather phenomenon with hotly debated dynamics. There is not even a generally accepted definition of polar lows. It is often assumed that the systems identified as polar lows include a spectrum "of mesoscale cyclones including both purely baroclinic as well as purely 'convective' systems, i.e.

systems for which the main energy source is latent heat release in deep convection'' (Rasmussen and Turner 2003, section 1.3). The focus of the present investigation is the convective systems and whether the release of preexisting CAPE can explain them. This should not be seen as reflecting the view that baroclinic instability is unimportant for cyclogenesis or indeed the maintenance of polar lows. On the contrary, we find it likely that baroclinic instability plays a nonnegligible role throughout the life cycles of all polar lows. This can be motivated by the rather strong horizontal temperature gradient characterizing the regions where polar lows exist, such as the Nordic Seas. To this we add that polar lows tend to be embedded in larger low pressure systems, which are baroclinic.

Nonetheless, polar lows are an exclusively marine phenomenon, which is an indication of the importance of the heat fluxes from the ocean, and researchers have

noted the apparent similarities between polar lows and tropical cyclones. Accordingly, theories for tropical cyclones have been used to try to explain polar lows. The intensities of tropical cyclones are to a large degree controlled by the energy content of the upper ocean. The depth of the mixed ocean surface layer and the entrainment of cooler water from below are critical factors (Emanuel et al. 2004; Hong et al. 2000; Shay et al. 2000). Saetra et al. (2008) showed that a corresponding warming of the mixed layer can occur in the Nordic Seas, which may influence the intensity of polar lows. Linders (2009), on the other hand, found a rather limited influence of the sea surface temperature in numerical simulations of polar lows. The conclusion should probably be that dealing with polar lows means dealing with two different and by themselves dynamically very complicated phenomena, namely baroclinic instability and tropical cyclone dynamics. One way to better understand such a complex system of phenomena is to make maximum use of observations.

A unique dataset of recent observations targeting polar lows has been analyzed here, allowing this study to shed some light on the characteristics of the atmosphere in and around polar lows. Two definite conclusions can be drawn:

1) Conditional instability is virtually nonexistent. Any sizable amount of conditional available potential energy (CAPE) is associated with (unconditional) instability and expresses a flux of energy rather than a reservoir.

2) Observed CAPE values are equivalent to the energy transfer from the ocean during a limited time (less than 1 h). It is therefore highly unlikely that the CAPE calculated at any given time represents any significant part of the energy budget of a polar low, integrated over a longer period. Once again, this is consistent with the CAPE expressing a flux of energy and not a reservoir.

According to Xu and Emanuel (1989), the tropical atmosphere does not contain any large amounts of CAPE and therefore cannot explain the development of tropical cyclones. Williams and Renno (1993), on the other hand, include the ice phase in their calculation of CAPE and come to the conclusion that the tropical atmosphere is definitely conditionally unstable. In the present investigation we show that over the Nordic Seas the CAPE is very limited and the developments of polar lows cannot be explained by the release of such a limited reservoir of energy.

The lack of any significant amount of CAPE in the observations considered here lead us to propose the hypothesis that this result is generally valid for the marine Arctic atmosphere. We propose that over open waters, the buildup of large reservoirs of CAPE is prevented by the onset of convection and CAPE is consumed more or less as rapidly as it is produced.

In this paper we abstain from taking a position on whether preexisting CAPE is a prerequisite for the CISK theory, or whether CISK can be a working mechanism for polar lows. However, we believe that the present investigation shows convincingly that preexisting CAPE cannot be a working mechanism for polar lows.

The role of baroclinic instability has only been briefly mentioned here. The polar low of 4 March is clearly baroclinic, but the extent to which this contributes to its forcing has not been assessed. Further investigations of polar low forcing should include this. The relationship and interaction between baroclinic instability and WISHE also needs to be revisited. The sequential view, in which baroclinic instability spins up the polar low and WISHE intensifies and maintains it, should perhaps be replaced with an approach in which these processes act more in tandem. It would be especially interesting to investigate whether the energy supply from the ocean can create baroclinic instability at a rate comparable to its consumption. If this were the case, it would give baroclinic instability a role similar to that of CAPE, as a temporary stage in the flux of energy from the ocean to the upper atmosphere.

REFERENCES

Charney, J. G., and A. Eliassen, 1964: On the growth of the hurricane depression. *J. Atmos. Sci.,* **21,** 68–75.

Craig, G. C., and H. R. Cho, 1988: Cumulus heating and CISK in the extra-tropical atmosphere. Part I: Polar lows and comma clouds. *J. Atmos. Sci.,* **45,** 2622–2640.

——, and S. L. Gray, 1996: CISK or WISHE as the mechanism for tropical cyclone intensification. *J. Atmos. Sci.,* **53,** 3528–3540.

Craven, J. P., R. E. Jewell, and H. E. Brooks, 2002: Comparison between observed convective cloud-base heights and lifting condensation level for two different lifted parcels. *Wea. Forecasting,* **17,** 885–890.

Emanuel, K. A., 1986: An air–sea interaction theory for tropical cyclones. Part I: Steady-state maintenance. *J. Atmos. Sci.,* **43,** 585–604.

——, and R. Rotunno, 1989: Polar lows as arctic hurricanes. *Tellus,* **41,** 1–17.

——, C. DesAutels, C. Holloway, and R. Korty, 2004: Environmental control of tropical cyclone intensity. *J. Atmos. Sci.,* **61,** 843–851.

Gray, S. L., and G. C. Craig, 1998: A simple theoretical model for the intensification of tropical cyclones and polar lows. *Quart. J. Roy. Meteor. Soc.,* **124,** 919–947.

Holton, J. R. Ed., 2004: *An Introduction to Dynamic Meteorology.* Academic Press, 535 pp.

Hong, X., S. W. Chanh, S. Raman, L. K. Shay, and R. Hodur, 2000: The interaction between Hurricane Opal (1995) and a warm core ring in the Gulf of Mexico. *Mon. Wea. Rev.,* **128,** 1347–1365.

Kalnay, E., and Coauthors, 1996: The NCEP/NCAR 40-Year Reanalysis Project. *Bull. Amer. Meteor. Soc.,* **77,** 437–471.

Linders, T., 2009: Polar low interaction with the ocean. Ph.D. thesis, University of Oslo, 83 pp.

Martin, C., 2007: ASPEN user manual. NCAR, 56 pp.

McDonald, W. F., 1942: On a hypothesis concerning the normal development and disintegration of tropical hurricanes. *Mon. Wea. Rev.,* **70,** 1–7.

Montgomery, M. T., N. Van Sang, R. K. Smith, and J. Persing, 2009: Do tropical cyclones intensify by WISHE? *Quart. J. Roy. Meteor. Soc.,* **135,** 1697–1714.

Økland, H., 1987: Heating by organized convection as a source of polar low intensification. *Tellus,* **37,** 397–407.

Rasmussen, E. A., 1979: The polar low as an extratropical CISK disturbance. *Quart. J. Roy. Meteor. Soc.,* **105,** 531–549.

——, and J. Turner, Eds., 2003: *Polar Lows.* Cambridge University Press, 612 pp.

Saetra, O., T. Linders, and J. B. Debernard, 2008: Can polar lows lead to a warming of the ocean surface? *Tellus,* **60A,** 141–153.

Shay, L., G. J. Goni, and P. G. Black, 2000: Effects of a warm oceanic feature on Hurricane Opal. *Mon. Wea. Rev.,* **128,** 1366–1382.

Smith, R. K., M. T. Montgomery, and S. Vogl, 2008: A critique of Emanuel's hurricane model and potential intensity theory. *Quart. J. Roy. Meteor. Soc.,* **134,** 551–561.

Van Sang, N., R. K. Smith, and M. T. Montgomery, 2008: Tropical-cyclone intensification and predictability in three dimensions. *Quart. J. Roy. Meteor. Soc.,* **134,** 563–582.

Williams, E. R., and N. Renno, 1993: An analysis of the conditional instability of the tropical atmosphere. *Mon. Wea. Rev.,* **121,** 21–36.

Xu, K.-M., and K. A. Emanuel, 1989: Is the tropical atmosphere conditionally unstable? *Mon. Wea. Rev.,* **117,** 1471–1479.